Correlation and relativistic effects on the photoionization of confined atoms

H. R. Varma,[1] P. C. Deshmukh,[1] V. K. Dolmatov,[2] and S. T. Manson[3]
[1]*Department of Physics, Indian Institute of Technology-Madras, Chennai, Tamil Nadu 600036, India*
[2]*Department of Physics and Earth Science, University of North Alabama, Florence, Alabama 35632, USA*
[3]*Department of Physics and Astronomy, Georgia State University, Atlanta, Georgia 30303, USA*
(Received 30 May 2007; published 18 July 2007)

A study of the combined effects of correlation, confinement and relativistic effects on the photoionization of the outer *ns* subshells of the alkaline-earth-metal atoms, Mg, Ca, Sr and Ba has been performed with particular emphasis on the Cooper minima using the relativistic-random-phase approximation (RRPA) methodology. It is found that the response of the Cooper minima to these various effects can be rather different behavior for the various atoms considered. On the other hand, relativistic effects were found to be essentially obliterated by confinement, in all cases. The situations are analyzed in detail and qualitative understanding of most of the phenomenology is presented.

DOI: 10.1103/PhysRevA.76.012711 PACS number(s): 32.80.Fb, 31.25.Eb

I. INTRODUCTION

There has been great interest in recent years in the properties of atoms confined in various environments, particularly in fullerene cages [1–4]. Aside from the interest from the basic physics point of view as to how the properties of the atom are altered by the conditions of the confinement, there is also considerable interest in possible applications of confined atoms in a wide variety of technological situations where nanostructures could be important. As an example, it has been shown that the fullerene cage is an ideal candidate for isolating the atom from the environment and, thereby, it provides a building block for the *q* bit of a quantum computer [5]. It is, thus, both of basic interest and applied importance to understand the change in the static and dynamic properties of confined atoms as compared to free atoms.

The response of a physical system to ionizing radiation, photoionization, is one of the most basic properties of nature. The cross section for photoionization depends sensitively upon the wave functions of the initial discrete and final continuum state of the target system. Thus, the study of photoionization of confined systems provides insight into the changes in both discrete and continuum wave functions engendered by the confinement. The presence of an external attractive confining potential tends to pull in the electron probability densities (both discrete and continuum), into the confining cage and, thereby, can bring about significant changes in the photoionization parameters. Both the energy spectra and electron occupancy of various subshells are sensitive to the parameters of confinement [2]. Photoionization studies of confined atoms have been carried out hitherto using theoretical tools because of the difficulties in producing such systems in concentrations large enough to carry out experimental investigations. However, this scenario is now changing; investigations on atoms or molecules confined in fullerene cages using synchrotron radiation are already under way [6].

In light of these developments, an investigation of the combined effect(s) of correlation, relativistic effects, and confinement upon the properties of atoms has been initiated. In this paper, we focus upon the dipole photoionization process and particularly on Cooper minima [7], zeros (or near zeros) in the relevant dipole matrix elements, since the photon energies at which they occur are known to be extremely sensitive to these various interactions [7]. As a first step, we report on the photoionization of the outer *ns* outer subshells of the alkaline earth atoms, Mg, Ca, Sr and Ba, confined endrohedrally in a C_{60} cage; these confined atoms are referred to as Mg@C_{60}, or just @Mg (when it is clear what the confining cage is), etc. The choice of *s* subshells was made because only $l \rightarrow l+1$ transitions are allowed, making the photoionization results most easily interpreted. We explore the outer valence subshells because they are the atomic electrons most affected by the confinement potential. Alkaline earth elements were chosen because they are closed-subshell atoms, which are simpler than open-subshell atoms, along with the fact that some nonrelativistic calculations have been reported on Mg and Ca, providing a convenient check on the extent of relativistic effects. In the calculations reported, we employ the relativistic random phase approximation (RRPA) since correlation, relativistic effects, and confinement can all be included on an *ab initio* basis. As far as we are aware, there are no previous studies of the combined effect(s) of correlation, relativity, and confinement effects on atomic photoionization.

In the next section, a brief discussion of the theoretical methodology is presented along with a presentation of the model potential used to approximate the C_{60} potential. In addition, some discussion of the change in the atomic binding energies and probability densities resulting from the confining potential is given in this section. The subsequent section presents and discusses the photoionization results, and the final section presents concluding remarks.

II. BRIEF THEORY AND METHOD OF CALCULATION

A. Confinement potential

A model potential for the confinement effects of the C_{60} cage, determined by fitting experimental data on the size and electron affinity of the C_{60} molecule [8], has been employed in the present calculations. The atom is assumed to be at the

TABLE I. Calculated threshold (binding) energies in a.u. for each of the occupied subshells of the free and confined alkaline earth atoms, along with the differences in the columns labeled Δ.

nlj	Mg	@Mg	Δ	Ca	@Ca	Δ	Sr	@Sr	Δ	Ba	@Ba	Δ
$1s$	49.1266	49.2621	0.135	150.1639	150.3026	0.1387	595.6307	595.7497	0.1190	1383.8012	1383.8906	0.0894
$2s$	3.7801	3.9082	0.1281	16.9674	17.1019	0.1355	83.1456	83.2634	0.1178	222.5733	222.6619	0.0886
$2p_{1/2}$	2.2883	2.4193	0.1310	13.7316	13.8688	0.1372	75.3760	75.4945	0.1185	209.0880	209.1770	0.0890
$2p_{3/2}$	2.2767	2.4077	0.1310	13.5925	13.7300	0.1375	72.8424	72.9609	0.1185	195.0103	195.0993	0.0890
$3s$	0.2534	0.3188	0.0654	2.2620	2.3893	0.1273	13.9596	14.0759	0.1163	48.6508	48.7389	0.0881
$3p_{1/2}$				1.3492	1.4785	0.1293	11.0781	11.1954	0.1173	42.9566	43.0452	0.0886
$3p_{3/2}$				1.3338	1.4630	0.1292	10.673	10.7903	0.1173	40.1673	40.2560	0.0887
$3d_{3/2}$							5.6286	5.7459	0.1173	30.2979	30.3866	0.0887
$3d_{5/2}$							5.5581	5.6755	0.1174	29.7119	29.8006	0.0887
$4s$				0.1963	0.2983	0.1020	1.9489	2.0582	0.1093	10.2571	10.3438	0.0887
$4p_{1/2}$							1.1264	1.2368	0.1104	8.0991	8.1867	0.0876
$4p_{3/2}$							1.0799	1.1900	0.1101	7.5132	7.6007	0.0875
$4d_{3/2}$										3.9136	4.0008	0.0872
$4d_{5/2}$										3.8126	3.9000	0.0874
$5s$							0.1813	0.2935	0.1122	1.6035	1.6842	0.0807
$5p_{1/2}$										0.9564	1.0378	0.0814
$5p_{3/2}$										0.8727	0.9534	0.0807
$6s$										0.1632	0.2873	0.1241

center of the fullerene cage. The potential is taken to be a spherical, attractive, annular potential well with an inner diameter $r_c=5.8$ a.u. from the center, having a thickness $\Delta=1.9$ a.u. and a depth $U_0=-8.22$ eV.

B. RRPA calculation

The RRPA methodology is employed herein. Since RRPA is based upon the Dirac equation, relativistic effects are included explicitly. In addition, RRPA includes significant aspects of multielectron correlation effects, including initial state correlation and interchannel coupling. The details of the RRPA methodology are discussed in detail elsewhere [9]. The existing RRPA methodology and codes [9] have been extended to include an external potential, such as the potential described above. Thus, it is emphasized, that the present investigation includes relativistic, correlation, and confinement effects on an *ab initio* basis; none of the effects are treated as perturbations.

Another useful feature of the RRPA methodology is that the number of interacting photoionization channels can be varied, i.e., the RRPA can be truncated. Of course, the calculation including coupling among *all* of the relativistic single-excitation channels arising from the photoionization of the ground state of the atom is the most accurate. Truncation provides insight into the effects of a specific coupling on the result; thus our calculations have been performed at different levels of truncation. Specifically, in each case, Mg, Ca, Sr, and Ba, we have performed calculations including just the two relativistic photoionization channels from the valence shell, $ns\rightarrow\varepsilon p_{1/2}$ and $ns\rightarrow\varepsilon p_{3/2}$; this calculation includes just *intrashell* coupling and amounts to a quasi-single-particle calculation. In addition, for each case, we have performed calculations including all photoionization channels coupled except those from the deepest subshells, which are too far removed energetically from the valence shell to be of nonnegligible influence on the valence photoionization cross section at low energies. In particular, along with the two valence ns channels described above, we have included Mg $(1s^22s^22p^63s^2)$: $2p_{3/2}\rightarrow\varepsilon s_{1/2}$, $\varepsilon d_{3/2}$, $\varepsilon d_{5/2}$, $2p_{1/2}\rightarrow\varepsilon s_{1/2}$, $\varepsilon d_{3/2}$, $2s\rightarrow\varepsilon p_{1/2}$, $\varepsilon p_{3/2}$; Ca $(1s^22s^22p^63s^23p^64s^2)$: $3p_{3/2}\rightarrow\varepsilon s_{1/2}$, $\varepsilon d_{3/2}$, $\varepsilon d_{5/2}$, $3p_{1/2}\rightarrow\varepsilon s_{1/2}$, $\varepsilon d_{3/2}$, $3s\rightarrow\varepsilon p_{1/2}$, $\varepsilon p_{3/2}$; Sr $(1s^22s^22p^63s^23p^63d^{10}4s^24p^65s^2)$: $4p_{3/2}\rightarrow s_{1/2}$, $\varepsilon d_{3/2}$, $\varepsilon d_{5/2}$, $4p_{1/2}\rightarrow\varepsilon s_{1/2}$, $\varepsilon d_{3/2}$, $4s\rightarrow\varepsilon p_{1/2}$, $\varepsilon p_{3/2}$, $3d_{5/2}\rightarrow\varepsilon p_{3/2}$, $\varepsilon f_{5/2}$, $\varepsilon f_{7/2}$, $3d_{3/2}\rightarrow\varepsilon p_{1/2}$, $\varepsilon p_{3/2}$, $\varepsilon f_{5/2}$, $3p_{3/2}\rightarrow\varepsilon s_{1/2}$, $\varepsilon d_{3/2}$, $\varepsilon d_{5/2}$, $3p_{1/2}\rightarrow\varepsilon s_{1/2}$, $\varepsilon d_{3/2}$, $3s\rightarrow\varepsilon p_{1/2}$, $\varepsilon p_{3/2}$; and Ba $(1s^22s^22p^63s^23p^63d^{10}4s^24p^64d^{10}5s^25p^66s^2)$: $5p_{3/2}\rightarrow\varepsilon s_{1/2}$, $\varepsilon d_{3/2}$, $\varepsilon d_{5/2}$, $5p_{1/2}\rightarrow\varepsilon s_{1/2}$, $\varepsilon d_{3/2}$, $5s\rightarrow\varepsilon p_{1/2}$, $\varepsilon p_{3/2}$, $4d_{5/2}\rightarrow\varepsilon p_{3/2}$, $\varepsilon f_{5/2}$, $\varepsilon f_{7/2}$, $4d_{3/2}\rightarrow\varepsilon p_{1/2}$, $\varepsilon p_{3/2}$, $\varepsilon f_{5/2}$, $4p_{3/2}\rightarrow\varepsilon s_{1/2}$, $\varepsilon d_{3/2}$, $\varepsilon d_{5/2}$, $4p_{1/2}\rightarrow\varepsilon s_{1/2}$, $\varepsilon d_{3/2}$, $4s\rightarrow\varepsilon p_{1/2}$, $\varepsilon p_{3/2}$; a total of 9 relativistic channels for Mg and Ca, along with 22 for Sr and Ba. In order to focus upon the effect(s) of the confinement on the photoionization process, all calculations are performed for both the confined atom and the free atom.

Note that RRPA employs Dirac-Fock (DF) wave functions [10] as the starting point, and uses DF binding energies throughout. Thus, it is of interest to scrutinize the DF binding energies and wave functions of the alkaline earth atoms to understand how the confinement potential alters them.

C. DF binding energies and wave functions

The threshold (binding) energies for the various subshells of the alkaline-earth-metal atoms are presented in Table I. Since the confining potential is attractive, the binding ener-

gies of the confined atoms must be larger than their free counterparts, and that is indeed seen; this is similar to what was seen in earlier studies of @Mg [11] and @Ca [3]. Of particular note is that the inner-shell energy differences, for each atom, remain almost exactly the same, irrespective of the subshell, i.e., the confinement increases all of the inner-shell binding energies by about the same amount. This can be understood by noting that, from Gauss' Law, a spherical annular electrostatic potential such as the confining potential of our model, exerts no force in the interior region. The only effect is to change the potential in the entire interior region by a constant amount, negative in this case since the confining potential is attractive. This shows that, to a good approximation, all of the inner-shell electron binding energies, for each atom, are lowered by the same amount. By the same arguments, the wave functions of these inner-shell electrons are unchanged. This same effect was seen in studies of the static and dynamic properties of inner-shell electron of atomic ions upon removal of outer-shell electrons [12].

Note that the lowering is not *exactly* the same for each inner shell because there is another factor involved. The calculated DF threshold energies are the result of a self-consistent field calculation wherein each atomic electron "feels" the direct and exchange effects of all of the other electrons. While the inner-shell electrons are "inside" the confining potential (i.e., in the region $r<r_c$), the valence ns electrons are not. Thus, they are strongly affected by the confining potential as seen in Table I by the very large percentage change in their binding energies. The differential direct and exchange effects of the valence electrons upon the inner-shell electrons account for the small differences in Δ among the inner shells of each atom. Since the effect upon the valence ns electrons differs for each Z, their effect on the inner shells vary, thereby explaining the differing Δ's for the various atoms. As a corollary, the inner-shell wave functions are actually altered, but only *very* negligibly.

There is one *caveat* to the above discussion, and this involves the $5s$ and $5p$ subshells of Ba. These are mostly, but not entirely inside the confining potential, so that they are not entirely inner shells in the sense of the above discussion. Thus, the change in their binding energies due to the confining potential is seen in Table I to be somewhat different (by about 10%) from the deeper inner shells.

Getting back to the valence ns subshells which "feel" the direct effects of the confining potential, these wave functions do, of course, change owing to the confinement. The probability densities (absolute squares) of these wave functions are shown in Fig. 1 as a function of radial distance; these are shown rather than the actual wave function in order to facilitate comparison of the multinodal wave functions among the various atoms. From Fig. 1, it is evident that, for the free atoms, the peak of the valence ns probability distribution (and wave function) moves to larger r with increasing Z, i.e., more of the valence ns electron density is in the region of the C_{60} cage with increasing Z. Hence, for the atoms in the confining potential, the valence ns probability density must be progressively affected more strongly, with increasing Z. Exactly this is seen in Fig. 1. The @Mg $3s$ radial probability density acquires a small hump in the vicinity of the cage, owing to the confining potential, but the maximum in the probability distribution is seen to remain well inside the cage, at about 3 a.u. For the other three cases, the overlap with the cage potential is strong enough that the maxima in the probability moves into the cage region, so that the wave functions and probability densities are dramatically altered by the confinement, as seen in Fig. 1. This shows that the response of the Mg $3s$ wave function to the confining potential is *qualitatively* different from Ca $4s$, Sr $5s$, and Ba $6s$. Furthermore, as expected, since the free atom valence ns wave functions are more diffuse with increasing Z, the strongest effect is on Ba $6s$, which shows the largest probability in the confining well.

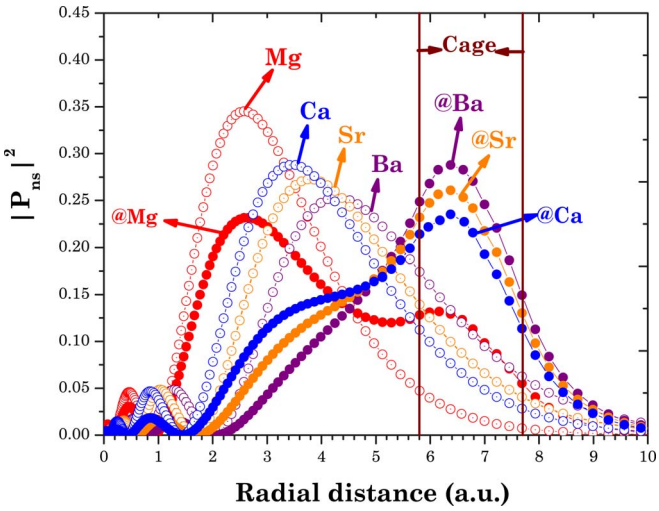

FIG. 1. (Color online) Valence ns radial electron probability densities $|\mathbf{P}_{ns}|^2$ for free (Mg, Ca, Sr, and Ba) and confined (@Mg, @Ca, @Sr, @Ba) alkaline-earth-metal atoms. The location of the model C_{60} cage potential is indicated by the vertical lines.

III. RESULTS AND DISCUSSION

Calculations have been carried out for the near-threshold photoionization of the outer ns subshell of both the free alkaline-earth-metal atoms, Mg, Ca, Sr and Ba, and the same atoms encapsulated in a C_{60} cage. In each case we performed a two-channel quasi-single-particle calculation, along with an RRPA calculation including all relativistic single-excitation channels, which might affect the valence ns cross section, as described in the previous section. For Mg, the lightest atom studied, the results are shown in Fig. 2, where it is seen that, for both Mg and $Mg@C_{60}$, the $3s$ photoionization cross section exhibits the effects of a Cooper minimum. In both cases, free and confined Mg, the effect of correlation in the form of interchannel coupling is to move the cross section minimum closer to threshold. Furthermore, the effect of confinement is to move the minima for $Mg@C_{60}$ to larger photoelectron energy, i.e., away from threshold, as compared to free Mg.

A previous theoretical study of $Mg@C_{60}$ has also looked at photoionization [11]. But this study emphasized autoionizing resonances, rather than the nonresonant background cross section. In addition, a rather different atomic model

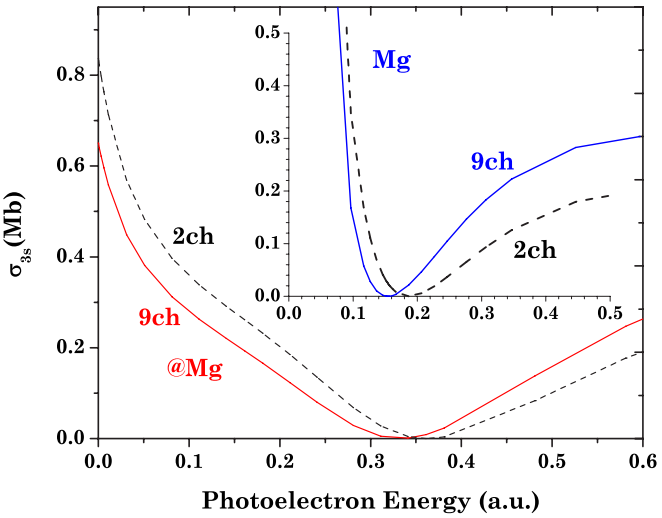

FIG. 2. (Color online) 3*s* photoionization of free Mg and @Mg as a function of photoelectron energy in atomic units (a.u.); 2ch and 9ch refer to the two-channel and nine-channel RRPA calculation, respectively. Continuous lines have more correlation (more interchannel coupling) than the dashed curves, as described in the text.

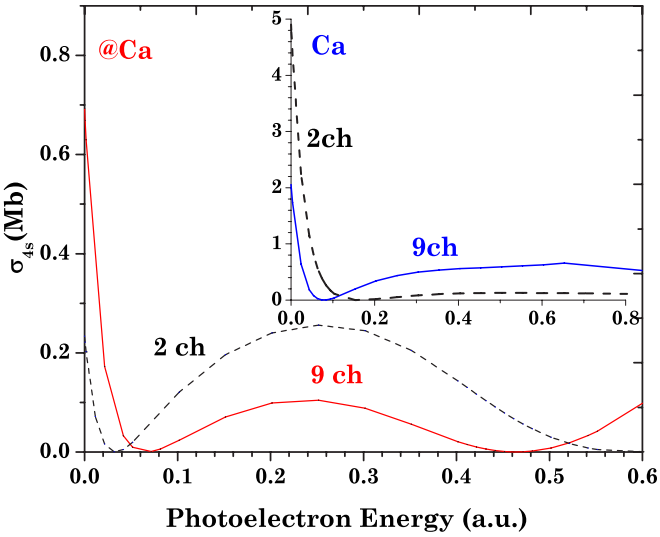

FIG. 3. (Color online) 4*s* photoionization of free Ca and @Ca as a function of photoelectron energy in atomic units (a.u.); 2ch and 9ch refer to the two-channel and nine-channel RRPA calculation, respectively. Continuous lines have more correlation (more interchannel coupling) than the dashed curves, as described in the text.

was employed, which included double excitations, but omitted interchannel coupling since a central potential was used to model the effects of the Mg^{+2} core upon the outer electrons. The only direct comparison that can be made is the threshold cross section for $Mg@C_{60}$ for which our result is about a factor of 2 larger than the results of Ref. [11]. Since it is unlikely that double excitations have any appreciable effect at threshold, the differences are attributed to differences in the potentials employed for the confining well, and the omission of interchannel coupling in the calculations of Ref. [11]. Since we have found interchannel coupling to be important, we suspect the present threshold cross section is more accurate than the result of Ref. [11].

For Ca, the next member of the alkaline-earth-metal column of the periodic table, the results are shown for Ca and @Ca in Fig. 3, where it is seen that the interchannel coupling moves the Cooper minimum to lower photoelectron energy for Ca, just like the Mg case, but to *higher* photoelectron energy for @Ca, just the opposite of the @Mg case. In addition, the confinement is seen to introduce a second (higher-energy) minimum in @Ca, which is moved to lower energy by interchannel coupling; this minimum is actually the result of a confinement resonance [13], a resonance resulting from the interference of the "direct" photoelectron wave, and the wave reflected from the confinement potential, and was found earlier in a nonrelativistic calculation [14].

Going up in *Z* to the next alkaline-earth-metal, the results are shown for Sr and @Sr in Fig. 4 where it is seen that, just like the case of Ca, interchannel coupling causes the Cooper minimum to move to lower photoelectron energy for the free atom, but higher energy for the confined @Sr. The magnitudes of the changes in the positions of the Cooper minima for both Sr and @Sr are seen to be larger than for the corresponding cases in Ca. The situation is similar for the heaviest alkaline-earth-metal considered here, Ba, shown in Fig. 5. However, for Ba and @Ba, interchannel coupling affects the Cooper minima much more strongly; for the free atom, the minimum in the cross section moves in to lower photoelectron energy by about half an a.u., while for @Ba, the minimum moves out to significantly larger energy. Thus, it is seen that for the free alkaline-earth-metal atoms, interchannel coupling always moves the minimum in the cross section to smaller photoelectron energy, and this change in energy increases substantially with *Z*. For their confined atom counterparts, the situation is more complicated; for @Mg interchannel coupling moves the minimum to lower energy, while for the rest of the series, the cross section minimum is moved

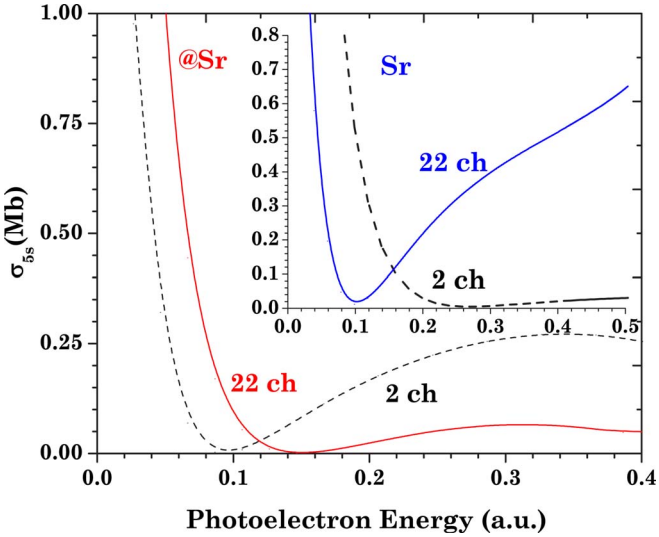

FIG. 4. (Color online) 5*s* photoionization of free Sr and @Sr as a function of photoelectron energy in atomic units (a.u.); 2ch and 22ch refer to the two-channel and 22-channel RRPA calculation, respectively. Continuous lines have more correlation (more interchannel coupling) than the dashed curves, as described in the text.

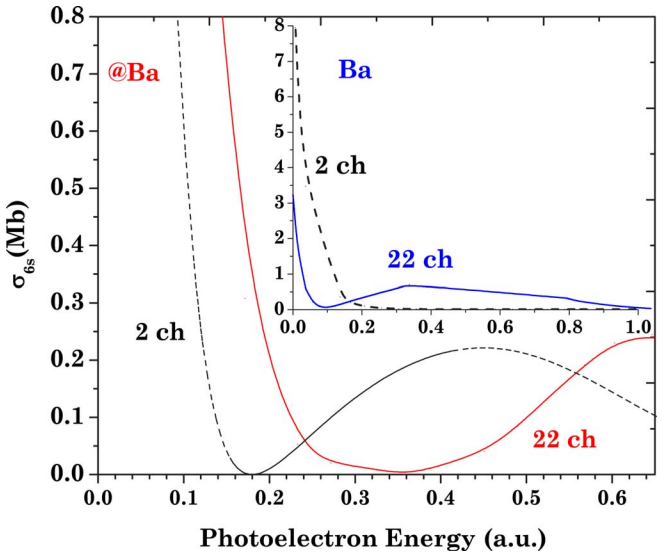

FIG. 5. (Color online) 6*s* photoionization of free Ba and @Ba as a function of photoelectron energy in atomic units (a.u.); 2ch and 22ch refer to the two-channel and 22-channel RRPA calculation, respectively. Continuous lines have more correlation (more interchannel coupling) than the dashed curves, as described in the text.

to higher energy, the increase in energy increasing with *Z*.

At this point, it is useful to note that the minima in the cross section that the Cooper minima, discussed above, are really sort of effective Cooper minima. This is because each cross section is the sum of the partial cross sections corresponding to the two (relativistic) photoionization $ns \rightarrow \varepsilon p_{3/2}$ and $ns \rightarrow \varepsilon p_{1/2}$; and relativistic effects can cause the Cooper minima in the two individual channels to differ, especially as *Z* increases. Thus, the above effective Cooper minimum is an amalgam of the two individual Cooper minima, in each case. To see this clearly, the positions of the individual Cooper minima are shown in Table II, and the results are rather surprising, in some respects. It is evident from the table that relativistic effects increase with *Z* for the free alkaline-earth-metal atoms for both the two-channel quasi-independent particle and correlated results. Except for a tiny separation for @Mg, the higher-*Z* confined atoms show no relativistic splitting of the Cooper minima at all, a result entirely contrary to the notion that relativistic effect should increase with *Z*.

Furthermore, the table shows the extremely complicated effect that the confinement has upon the locations of the individual Cooper minima. For Mg, confinement moves the Cooper minimum to larger photoelectron energy, for both two-channel and nine-channel calculations. For Ca, just the opposite is the case, with the two-channel results moving much more than the nine-channel. For Sr, confinement moves the two-channel Cooper minima to considerably lower energy, but the 22 channel is moved out somewhat. For Ba, like Sr, the two-channel Cooper minima are moved to lower energy by confinement, but the 22 channel move out.

Now that the phenomenology has been elucidated, it remains to try to understand how this phenomenology comes about. We focus first upon the effect(s) of correlation. The

TABLE II. Photoelectron energy positions of the Cooper minima in a.u. (27.21 eV) calculated for the free and confined alkaline-earth-metal elements.

	Mg		@Mg	
	2ch	9ch	2ch	9ch
$3s \rightarrow p_{3/2}$	0.1876	0.1546	0.3632	0.3332
$3s \rightarrow p_{1/2}$	0.1846	0.1526	0.3602	0.3312
Difference	0.0030	0.0020	0.003	0.0020
	Ca		@Ca	
	2ch	9ch	2ch	9ch
$4s \rightarrow p_{3/2}$	0.1647	0.0807	0.0337	0.0667
$4s \rightarrow p_{1/2}$	0.1537	0.0747	0.0337	0.0667
Difference	0.0110	0.0060	0	0
	Sr		@Sr	
	2ch	22ch	2ch	22ch
$5s \rightarrow p_{3/2}$	0.2977	0.1087	0.0935	0.1475
$5s \rightarrow p_{1/2}$	0.2127	0.0817	0.0935	0.1475
Difference	0.0850	0.0270	0	0
	Ba		@Ba	
	2ch	22ch	2ch	22ch
$6s \rightarrow p_{3/2}$	0.5638	0.1088	0.1797	0.3577
$6s \rightarrow p_{1/2}$	0.2128	0.0558	0.1797	0.3577
Difference	0.351	0.0530	0	0

fundamental effect of correlation is interchannel coupling since ground state correlation is already included in the two-channel quasi-single-particle calculation. Using the convention that all wave functions have positive slope at the origin, the dipole matrix element for the outer *ns* photoionizing transitions are negative at threshold, and change sign at the Cooper minimum; in fact, this change of sign is the basic cause of the Cooper minimum. The main interchannel coupling occurs with the channels arising from the next inner $(n-1)p$ channels, none of which has a Cooper minimum. Thus for the free atoms, from the Fano formalism [15], if the interchannel coupling matrix elements are negative (as they almost surely are owing to the overlap of the continuum wave functions differing by one unit of orbital angular momentum), since the energy denominator is negative, the dipole matrix elements are incremented by a positive amount, which pushes the Cooper minimum to lower energies. Since the inner $(n-1)p$ photoionization cross sections increase with *Z* (indicating that the associated dipole matrix elements also increase with *Z*), the effect of interchannel coupling should increase with *Z* as well; this is indeed seen in Table II.

The effect of correlation for @Mg, whose discrete wave function does not move much due to the confinement, is substantially the same as for free atoms. For the other confined atoms, their outer *ns* wave functions are moved out

considerably by the confinement, leading to a change of sign of the interchannel coupling matrix element, owing to the overlap of the discrete ns wave function with $(n-1)p$ (which is now negative) so that the interchannel coupling has just the reverse effect and moves the Cooper minima to higher energy in each of these cases. Furthermore, this effect increases with increasing Z for the same reason that the effect increased with Z for the free atoms. Thus, we have a general understanding of the physics underlying the effect(s) of interchannel coupling on both the free and confined atoms.

Looking next at relativistic effects, it is evident that for free atoms the relativistic splitting of the Cooper minima increase with Z owing to the increase of relativistic (spin-orbit) effects with Z. For @Mg, whose wave function does not move very much under confinement, the situation is similar to the free atom. For the others, the initial state wave function is moved out considerably by confinement, so that the spin-orbit interaction, which goes as $1/r^3$, is much smaller and does not affect the Cooper minima very much at all. Thus, the seemingly anti-intuitive behavior of relativistic effects for the higher-Z confined atoms results simply from the confinement-induced alteration of their outer ns wave functions moving the probability density to larger distance from the nucleus.

The effects of confinement on the Cooper minima are extremely complicated, as discussed above. We note that the nodes of the continuum wave function always move in towards the nucleus with increasing energy, and the Cooper minimum occurs where it has moved in just enough that the negative and positive contributions to the dipole matrix element just cancel. Thus, it is evident that from a single-particle (or quasi-single-particle) viewpoint, the change in the location of the Cooper minimum due to confinement depends critically upon the relative contraction (or elongation) of the initial discrete wave function vs the threshold final continuum wave function. Looking at Table II, it is seen that for Mg, confinement moves the two-channel (quasi-single-particle) Cooper minima to larger energy. Since the discrete Mg $3s$ wave function is elongated (moves out) a bit, then the threshold continuum wave function moves out even more, under the action of the confining potential well. For Ca and the higher Z members of the series, the discrete ns wave functions were seen to move out a great deal under confinement, clearly more than the threshold continuum wave functions, leading to the lowering of the energy of the Cooper minima, as seen.

For the highly correlated results, the situation is still more complicated because, in addition to the effects described above, there is also the effect(s) on the confinement upon the interchannel coupling. To understand this, in turn, requires understanding how the confining potential well affects both the interchannel coupling matrix elements, along with the dipole matrix elements for the $(n-1)p$ photoionization channels. Without going into detail here, suffice it to say that a simple qualitative explanation for the complicated behavior—with the Cooper minima moving to lower energy for Ca but higher energy for the others—has not been found.

IV. CONCLUDING REMARKS

Using the alkaline-earth-metal atoms Mg, Ca, Sr, and Ba as examples, a theoretical study of the combined effects of correlation, relativity, and confinement within a C_{60} cage has been performed concentrating upon the photoionization of the valence ns subshell in each case. In particular, the investigation focused on the Cooper minima, zeros (or near zeros) in the continuum dipole matrix elements and it was found that their energy positions are extremely sensitive to these various interactions. Furthermore, the behavior of the Cooper minima was found to be exceedingly complicated; nevertheless, qualitative explanations were found for a large portion of the phenomenology encountered.

The investigation employed the relativistic-random-phase approximation (RRPA), which takes into account both initial state correlations, interchannel coupling, and relativistic effects in an *ab initio* manner. RRPA does not, however, take multielectron ionization-plus-excitation (satellite processes) into account [9] so that the calculation is somewhat inaccurate in any region where such processes are important. Nevertheless, despite this omission, it is useful to employ a relativistic calculation for a number of reasons. Although the outer shells are not relativistic, for the heavier systems (particularly Ba) the inner shells are, and the change in their charge distribution affects the outer shell. In addition, the splitting of Cooper minima in a closed subshell system can only be effected by relativistic interactions; no amount of correlation can cause such splittings. Furthermore, past experience has indicated that relativistic effects influence a variety of nonrelativistic results similarly, from central-field to highly correlated approximations [16]; thus, the present inclusion of these relativistic effects is instructive, irrespective of the level of correlation included. Finally, the fact that the two-electron autoionizing resonances sometimes occur in the energy regions of Cooper minima certainly changes the cross section in these regions. This makes the Cooper minima more difficult (but not impossible) to locate. Past experience has shown, however, that resonances in the vicinity of Cooper minima do not appreciably change the location or character of these minima [17] and that the RRPA results for outer shells show excellent agreement with experiment [18]. Thus, it is expected that the present Cooper minima results for confined atoms are reasonably accurate. In any case, in future work, we hope to ameliorate this omission of satellite processes, both resonant and nonresonant, by applying a multiconfigurational RRPA methodology to the problem.

ACKNOWLEDGMENTS

This work was partially supported by BRNS, DAE (India), DST (India), NSF (USA), and DOE (USA). The authors are indebted to Walter Johnson for the use of his codes and for his assistance in modifying them.

[1] W. Jaskolski, Phys. Rep. **271**, 1 (1996).
[2] J. P. Connerade, V. K. Dolmatov, P. A. Lakshmi, and S. T. Manson, J. Phys. B **32**, L239 (1999).
[3] V. K. Dolmatov, A. S. Baltenkov, J.-P. Connerade, and S. T. Manson, Radiat. Phys. Chem. **70**, 417 (2004), and references therein.
[4] C. H. Turner, J. K. Johnson, and K. E. Gubbins, J. Chem. Phys. **114**, 1851 (2001).
[5] W. Harneit, Phys. Rev. A **65**, 032322 (2002).
[6] R. Phaneuf (private communication).
[7] A. F. Starace, in *Handbuch der Physik*, edited by W. Mehlhorn (Springer-Verlag, Berlin, 1982), Vol. 31, pp. 1–121, and references therein.
[8] Y. B. Xu, M. Q. Tan, and U. Becker, Phys. Rev. Lett. **76**, 3538 (1996).
[9] W. R. Johnson and C. D. Lin, Phys. Rev. A **20**, 964 (1979).
[10] I. P. Grant, *Relativistic Quantum Theory of Atoms and Molecules: Theory and Computation*, Springer Series on Atomic, Optical, & Plasma Physics (Springer-Verlag, New York, 2006), p. 325 ff., and references therein.
[11] A. Lyras and H. Bachau, J. Phys. B **38**, 1119 (2005).
[12] S. T. Manson, in *The Physics of Electronic and Atomic Collisions*, edited by A. Dalgarno, R. S. Freund, P. M. Koch, M. S. Lubell, and T. B. Lucatorto, AIP Conf. Proc. No. 205 (AIP, New York, 1990), pp. 189–200.
[13] J.-P. Connerade, V. K. Dolmatov, and S. T. Manson, J. Phys. B **33**, 2279 (2000).
[14] J.-P. Connerade, V. K. Dolmatov, and S. T. Manson, J. Phys. B **32**, L395 (1999).
[15] U. Fano, Phys. Rev. **124**, 1866 (1961).
[16] A. Ron, I. B. Goldberg, J. Stein, S. T. Manson, R. H. Pratt, and R. Y. Yin, Phys. Rev. A **50**, 1312 (1994), and references therein.
[17] H. Wang, G. Snell, O. Hemmers, M. M. Sant'Anna, I. Sellin, N. Berrah, D. W. Lindle, P. C. Deshmukh, N. Haque, and S. T. Manson, Phys. Rev. Lett. **87**, 123004 (2001).
[18] W. R. Johnson and K. T. Cheng, Phys. Rev. A **20**, 978 (1979).